FULL PAPER

# Stimuli-Free Reversible and Controllable Loading and Release of Proteins under Physiological Conditions by Exponentially Growing Nanoporous Multilayered Structure

*Weiyong Yuan, Zhisong Lu, Huili Wang, and Chang Ming Li**

**A unique delivery system to reversibly and controllably load and release proteins under physiological conditions is desirable for protein therapeutics. We fabricate an ultrafast exponentially growing nanoporous multilayer structure comprised of two weak polyelectrolytes, poly(ethyleneimine) and alginate with thickness and chemical composition controlled by the assembly pH. For the first time, the assembled multilayered structure demonstrates stimuli-free reversible protein loading and release capability at physiological conditions by a synthetic material. The protein loading and release time can also be controlled by the assembled bilayer number. The highest loading capacity for the target protein and longest release time of proteins for layer-by-layer films reported to date have been achieved with a 15-bilayered film fabricated in this work. The prominent properties of the assembled film provide great potential for various biomedical applications, especially as a delivery system for protein therapeutics.**

## 1. Introduction

Mimicking biological systems to design smart materials has recently attracted great interest.[1–6] Protein association and dissociation is a delicate process requiring high reversibility, a sufficient amount of protein, and fine control at the molecular level in various essential biological systems, including gene expression, cell metabolism, and signal transduction.[7–9] The fabrication of artificial systems with the capability of reversible loading and release of proteins is desirable for applications such as drug delivery,[10–12] protein separation,[13,14] biosensing,[15,16] biocatalysts,[17] and stimuli-responsive membranes.[18] In particular, such systems are very promising in protein therapeutics due to their capacity to maximize protein loading and release efficiency as well as to enhance bioavailability.[12,19,20] Although some efforts have been made to develop controlled protein release systems with reversibility, all existing reports use severe stimuli such as drastic change of pH, high ionic strength, or specific chemical exchangers, which are significantly different from the physiological conditions (pH approximately 7.4, ionic strength of around 150 mM, and temperature apporximately 37 °C), to render the thorough release of loaded proteins.[11,17,21,22] It is apparent that systems with stimuli at non-physiological conditions are not suitable for biological applications requiring protein activities to be maintained.[23–26] Functional materials that can reversibly and controllably load and release proteins under physiological conditions has not been realized so far.

Several challenges remain in designing a material with high protein loading capacity and stimuli-free loading/release reversibility under physiological conditions: i) increasing material surface area for high protein loading could introduce high protein retaining by non-specific adsorption and/or entrapment;[27–29] ii) enhancing affinity for protein loading can reduce the loading/release reversibility;[30,31] and iii) repeated immersions of materials in physiological environment deteriorates the loading capacity and reversibility.[32,33]

Nanostructured materials, in particular a nanoporous structure, could provide large surface area for high protein loading capacity, but a fundamental limitation of reported nanoporous systems is the easy entrapment of proteins inside the nanoporous structure, which greatly hinders the release of proteins and influences the reversibility.[29,34,35] Recently, exponentially growing layer-by-layer (e-LbL) self-assembly, in which the thickness of the assembled multilayers increases exponentially with increase of the bilayer number, has emerged as a versatile method to fabricate nanostructured thin films with unique properties.[36–41] In particular, the assembled nanostructure is a dynamic equilibrium system with a significant content of mobile uncomplexed building blocks.[30,38,39,41,42] Furthermore, the multilayer parameters, such as chemical composition, can be controlled through the assembly conditions[30,36,38,43–45] to provide a wide space to tune the affinity between the film and

Dr. W. Yuan, Dr. Z. Lu, Prof. C. M. Li
Institute for Clean Energy & Advanced Materials
Southwest University
Chongqing 400715, P. R. China
School of Chemical & Biomedical Engineering
and Center for Advanced Bionanosystems
Nanyang Technological University
70 Nanyang Drive, Singapore 637457, Singapore
E-mail: ecmli@ntu.edu.sg
Dr. H. Wang
School of Mechanical and Aerospace Engineering
Nanyang Technological University
50 Nanyang Avenue, Singapore 639798, Singapore

DOI: 10.1002/adfm.201102308

proteins. In addition, the e-LbL self-assembly can be performed in physiologically buffered solutions to obtain physiologically stable systems.[46,47] Thus, exponentially grown nanoporous structures could be good candidates for reversible and controllable loading and release of proteins under physiological conditions. However, to the best of our knowledge, there is no report on using self-assembled nanoporous films for reversible protein loading and release. Furthermore, the loading capacity, reversibility and controllability, all of which are important for the practical applications of such systems, have not been investigated.

In this work we investigated the pH-controlled e-LbL self-assembly of two weak polyelectrolytes, poly(ethyleneimine) PEI and alginate in phosphate buffered saline (PBS) solution and observed a nanoporous multilayer structure. We further explored the possibility of using this nanoporous multilayer structure for stimuli-free reversible protein loading and release in PBS solution (pH 7.4, 137 mM NaCl), a physiological condition.[25,26] The mechanism of the reversible loading and release of protein was studied based on the experimental results. The controllability of protein loading and release was also investigated.

## 2. Results and Discussion

### 2.1. Buildup and Characterization of Exponentially Growing Nanoporous Multilayers

The thickness evolution of the assembly process of PEI/alginate multilayers was tracked by cross-section field emission scanning electron microscopy (FE-SEM; **Figure 1**), showing that the thickness grows exponentially with the bilayer number at all studied assembly pHs (three representative pHs were chosen for demonstration). For a film with the same number of bilayers, the thickness first decreases then increases as the assembly pH rises (Figure 1, inset). This trend can be ascribed to the intrinsic nature of the weak polyelectrolytes. The charge density of PEI ($pK_a$ is a broad pH range of 6–9) decreases with the increased assembly pH[30,48] while alginate ($pK_a$ is between 3.4 and 3.7)[49] is fully charged at pH 5 or higher. Thus, at higher assembly pHs more PEI with a loopier structure is assembled to overcompensate the bulk charges of multilayer for increasing the thickness.[43,50] However, at lower assembly pHs, close to the $pK_a$ of alginate, the charge density of alginate decreases with decrease of the assembly pH, resulting in increased alginate assembly to overcompensate the multilayer charges.[43,50] That is why the assembly thickness increases with the pH decrease from pH 5. It is notable that PBS solution can greatly affect the assembly of PEI/alginate multilayers. The multilayer assembled in water shows a nearly negligible growth compared to that assembled in PBS with a similar pH (Figure S1, Supporting Information). The ultrafast thickness growth of the multilayers in PBS should be due to the high ionic strength, which enhances the film growth.[42,51] The PBS-involved assembly process may provide the film a high stability under physiological conditions, which is vital to a reversible protein loading and release system.

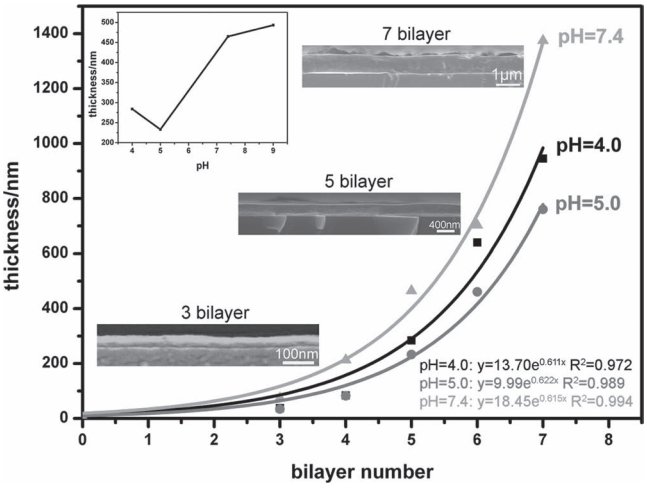


**Figure 1.** Thickness of the exponentially growing multilayers versus bilayer number. The thicknesses are obtained from the cross-section FESEM images, and fitted using exponential growth equations given below the curves. Insets show 5-bilayer films thickness evolution with assembly pH, and cross-section FESEM images of 3, 5, and 7-bilayer multilayers assembled at pH 5.

To explore the mechanism of exponential growth, the self-assembly process was tracked by cross-section confocal laser scanning microscopy (CLSM; **Figure 2**). After one layer of fluorescein isothiocyanate labeled PEI (FITC-PEI) is assembled on the top of PEI/alginate multilayers, the whole film becomes green, indicating FITC-PEI has diffused into the multilayers. Furthermore, after an $(alginate/PEI)_{2.5}$ multilayer is further assembled on top, the green color can be observed throughout the film including the outermost part, indicating FITC-PEI can diffuse out during the self-assembly. Such an in-and-out diffusion can result in assembled polyelectrolyte amount proportional to the film thickness in each step, thus leading to an exponential growth of multilayers.[37,40,42] In comparison to reported exponentially growing systems, such as chitosan (CH)/hyaluronan (HA),[52] poly(L-glutamic acid) (PGA)/poly(allylamine) (PAH),[53] and poly(L-lysine) (PLL)/HA,[54] assembled at a similar pH and ionic strength, ours has much faster thickness growth. The ultrafast thickness growth of our multilayers should be due to the strong interdiffusion ability of PEI and appropriate intermolecular interaction between PEI and alginate.[30,41]

The ultrafast exponential growth with strong molecule interdiffusion during self-assembly could spontaneously produce unique nanostructures.[36,43,44] The surface morphology

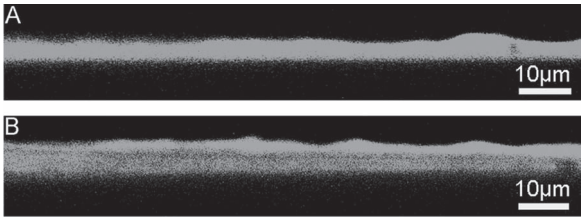


**Figure 2.** Cross-section CLSM images of: A) $(PEI/alginate)_{15}$ with one layer of FITC-PEI assembled on top, and, B) $(PEI/alginate)_{15}$ with one layer of FITC-PEI and 2.5 bilayer of alginate/PEI assembled on top.

of the films assembled at different assembly pH in dry state (**Figure 3**A–C) shows a large-area uniform nanoporous structure of the multilayer films. The pore size for all the films is smaller than 20 nm, which is the smallest for all reported self-assembled nanoporous multilayers.[35] To examine whether this nanoporous structure is still retained in a wet state for potential practical applications, the morphology of the film in PBS solution was investigated by cryo-transmission electron microscopy (Cryo-TEM) (Figure 3D, the film assembled at pH 5.0), which exhibits uniform nanopores, as observed in the dry state. The retained nanoporous structure in solution state indicates that proteins can also penetrate into the film to achieve very high loading capacity, see the later discussion. In comparison, LbL self-assembly of PEI and alginate at similar assembly pH in deionized (DI) water only shows nonporous morphology (Figure S2, Supporting Information).

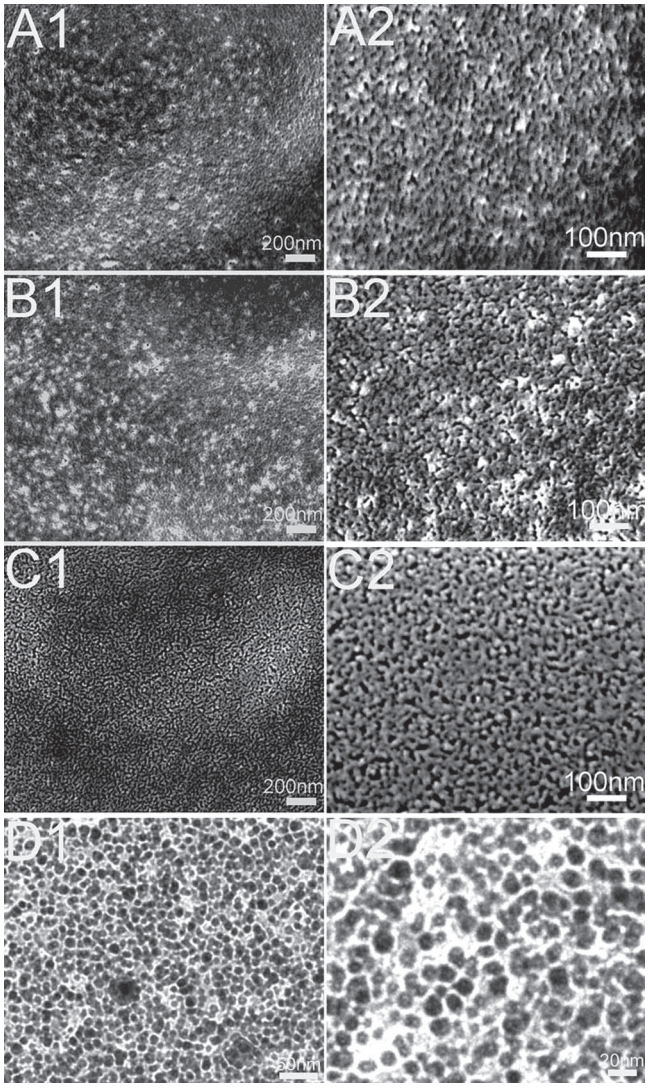


**Figure 3.** Low and high magnification FE-SEM images of PEI/alginate multilayers with 5 bilayers assembled at pH 4.0 (A1, A2), 5.0 (B1, B2), and 7.4 (C1, C2). Low and high magnification Cryo-TEM images of PEI/alginate multilayers with 5 bilayers assembled at pH 5.0 (D1, D2).

Fourier transform infrared (FTIR) spectroscopy was used to examine the evolution of chemical composition of the multilayers during assembly.[55,56] The FTIR spectra of PEI, alginate, and the multilayers assembled at pH 5 (**Figure 4**a; see Figure S3 and S4, Supporting Information, for FTIR spectra

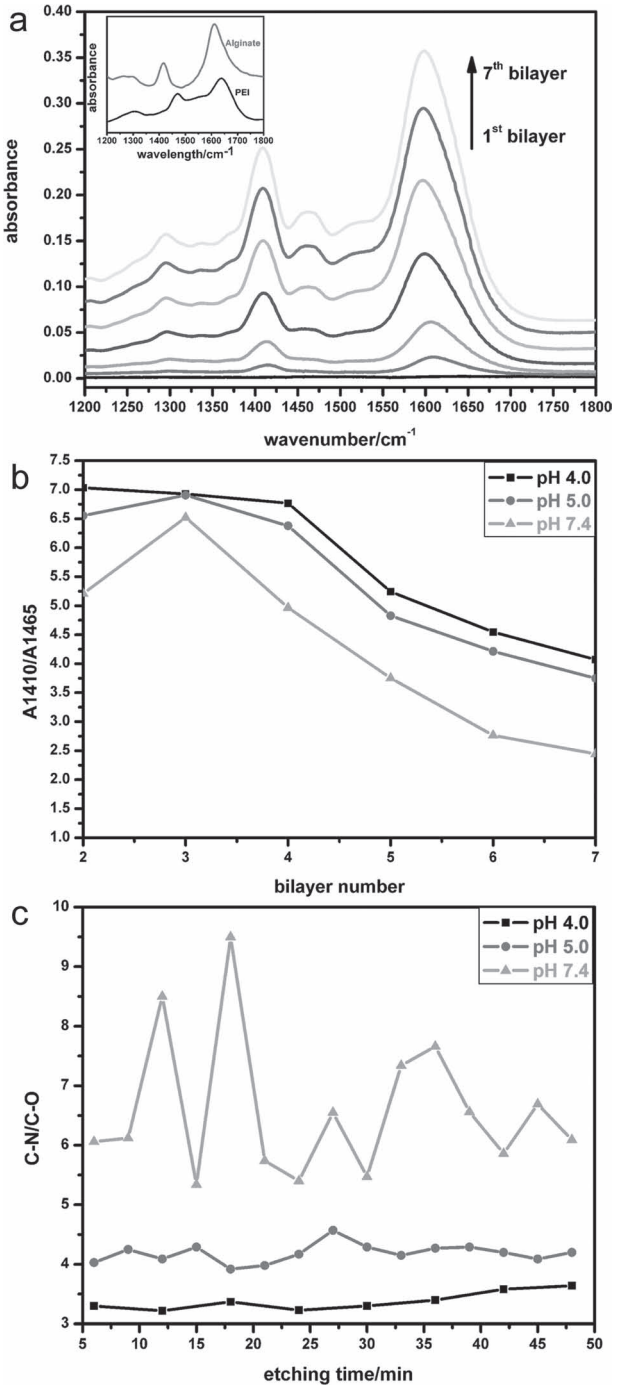


**Figure 4.** a) FTIR spectra of PEI/alginate multilayers with different bilayer number assembled at pH 5. Inset shows the FTIR spectra of PEI and alginate. b) Integrated peak intensity ratio of peak at around 1410 $cm^{-1}$ to that around 1465 $cm^{-1}$ of multilayers with different bilayer number and assembly pH. c) XPS depth profile of $(PEI/alginate)_5$ multilayers assembled at different assembly pH.

of multilayers assembled at other pHs) show characteristic peaks at around 1612 and 1416 $cm^{-1}$ of alginate (Figure 4a inset) from symmetric $COO^-$ stretching vibrations and asymmetric $COO^-$ stretching vibrations, respectively,[57] and at around 1639 and 1471 $cm^{-1}$ of PEI (Figure 4a inset) from N–H bending vibrations and $CH_2$ bending vibrations, respectively.[38,58] After the self-assembly (Figure 4a), the peaks at around 1416 and 1471 $cm^{-1}$ shift to around 1410 and 1465 $cm^{-1}$, respectively, due to the intermolecular interaction between PEI and alginate. Furthermore, a new peak at around 1599 $cm^{-1}$ is observed, possibly due to the coupling of peaks at 1639 and 1612 $cm^{-1}$. The characteristic peaks at around 1410 and 1465 $cm^{-1}$ display only a slight shift with the change of the assembled bilayer number and the assembly pH (Figure 4a, Figure S3 and S4, Supporting Information). The integrated peak intensities at around 1410 and 1465 $cm^{-1}$ calculated from deconvoluted spectra of the multilayers (see Figure S5 and S6, Supporting Information, for typical fitting curves) indicate exponential growth of the multilayered film with increase of the bilayer number (Figure S7, Supporting Information), which is in agreement with cross-section FE-SEM results. More importantly, the integrated intensity ratios of the peak around 1410 $cm^{-1}$ to that around 1465 $cm^{-1}$ (A1410/A1465) for multilayers with different bilayer number (Figure 4b) illustrate a significant decrease with increase of the assembly pH for each group of films with the same bilayer number from the second bilayer, indicating that the chemical composition of the multilayers can be easily tuned by changing the assembly pH, and that the amount of alginate relative to PEI reduces with increase of the assembly pH (considering that there are still some COOH groups at pH 4, this trend should be more obvious). The pH-controllable chemical composition of the film is due to charge overcompensation during the assembly. The charge density of PEI decreases with increasing assembly pH in the studied pH range, and that of alginate firstly increases at pH near its $pK_a$, then remains stable with further increase of pH. Thus, more alginate is needed to be assembled to overcompensate the charge of PEI at higher assembly pH, resulting in a lower PEI/alginate ratio.[42,43,50] It is noted that for each assembly pH, the ratio of alginate to PEI decreases with increase of the bilayer number from the third bilayer. The reason for this is not clear and is under investigation in our lab.

Depth-profiling X-ray photoelectron spectroscopy (XPS) was performed to further examine the chemical composition of the exponentially growing multilayered films assembled at different pHs. The C–N and C–O concentrations obtained from the fitting of carbon peaks are used to quantify the relative composition of PEI to alginate (Figure 4c, see Figure S8 and S9, Supporting Information, for typical fitting curves). The PEI/alginate ratio increases with increasing the assembly pH, which further supports the FTIR spectroscopy data.

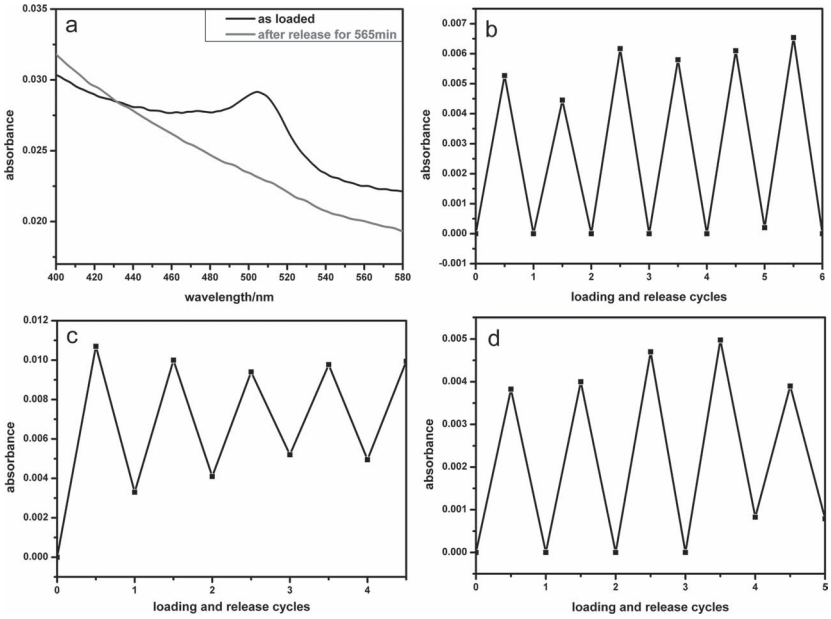


**Figure 5.** UV-vis spectra of BSA loaded PEI/alginate multilayers (5 bilayer, assembly pH 5.0) before and after release (a). UV-vis adsorption of repeated FITC-BSA loading and release for the 5-bilayer PEI/alginate multilayers assembled at assembly pH 5.0 (b), 7.4 (c), and 4.0 (d), after baseline correction.

### 2.2. Reversible Protein Loading and Release

The protein loading and release behavior of the PEI/alginate multilayers was further studied using bovine serum albumin (BSA), a frequently used model protein for protein release,[59,60] as a probe. **Figure 5**a shows the UV-visible (UV-vis) spectra of 5-bilayer multilayers assembled at pH 5.0 before and after release. An obvious UV-vis absorption peak around 506 nm is observed after immersion in fluorescein isothiocyanate labeled BSA (FITC-BSA) PBS solution for 12 h and thorough washing, indicating successful loading of FITC-BSA. After several hours exposure to PBS, the absorption peak disappears completely, indicating thorough release of proteins. The thorough release of FITC-BSA can be further demonstrated by the hardly detectable fluorescence signal of the multilayers after release (Figure S10, Supporting Information). The multiple loading and release experiment (Figure 5b) reveals that the FITC-BSA can be loaded to around the same level of first loading, followed by thorough release, and can be cycled many times without any amplitude attenuation, demonstrating excellent reversibility of loading and releasing. Importantly, there is no outer stimulus exerted. For the first time, a synthetic material to realize the reversible loading and release at physiological condition is accomplished. Further assembly of the film at other pHs shows that the loading capacity of FITC-BSA with film assembled at pH 7.4 is larger than that assembled at pH 5.0. However, there is significant retention of the protein (around 31% of UV-vis peak intensity remains) in the multilayered film after reaching the release plateau during the releasing process (Figure 5c, see Figure S11, Supporting Information, for UV-vis spectra before and after release of the multilayer assembled at pH 7.4). The reversibility of multilayer film assembled at pH 4.0 is also good,

although it slightly deteriorates from the fourth cycle of loading and release, which is possibly due to the poorer stability of the multilayer in pH 7.4 PBS (Figure 5d). The reversibility was also tested for the 15-bilayer film assembled at pH 5, showing that approximately 90% of the loaded protein can be released and can be reversibly loaded to the same level followed by around 86% release in the second releasing experiment. This reversibility is still reasonably good, although it is relatively poorer than for the 5-bilayer film. The slight protein retention in the 15-bilayer film is possibly due to defects introduced by the increased thickness, but the exact reason is still not very clear.

The exponentially growing film is a dynamic equilibrium system, in which the binding intensity between oppositely charged polyelectrolytes is weak enough to incorporate a significant loopy and mobile polymer chains inside.[38,39,61,62] For this model system, the dynamic equilibrium equation can be represented as

$$\text{PEI} + \text{alginate} \Leftrightarrow \text{PEI} : \text{alginate} \quad (1)$$

where PEI : alginate represents the polyelectrolyte complex of PEI and alginate, and PEIand alginate represent mobile uncomplexed polyelectrolytes in multilayers. The counterions associated with the free mobile polyelectrolyte are omitted here for convenience and the stoichiometric ratio is assumed as 1:1. Since BSA is negatively charged in pH 7.4 PBS, the positively charged mobile PEI is able to bind BSA as

$$\text{PEI} + \text{BSA} \Leftrightarrow \text{PEI} : \text{BSA} \quad (2)$$

During the loading process, Reaction 2 favors the right side due to the penetration of high concentration of BSA to the nanoporous film (will be further discussed). The existence of free mobile PEI is a driving force to load BSA as demonstrated by the pH-controlled loading experiment (Figure 5), in which a higher assembly pH results in a higher BSA loading. The multilayers assembled at a higher assembly pH have a higher ratio of PEI to alginate and more amount of mobile PEI, thus will load more BSA into the multilayers. In contrast, little BSA can be loaded in linearly growing multilayers with a dense structure and very little mobile polyelectrolyte, as shown in the typical linearly growing system discussed below. One could wonder whether negatively charged alginate is released or replaced during the BSA loading. FTIR spectroscopy results show that the spectra and the fitting peak at around 1410 $cm^{-1}$ (Figure S12 and S13, Supporting Information) for films assembled at pH 5.0 and 4.0 change insignificantly after thorough release of BSA in comparison to that before BSA loading, indicating no significant alginate molecules are released or replaced during BSA loading. Although the alginate release in film assembled at pH 7.4 is difficult to track due to BSA retention, we can reasonably argue that alginate is even harder to be replaced or released since it has equal and stronger negative charge than that at pH 5.0 and 4.0, while BSA possesses the same. When the protein-loaded multilayers are immersed in PBS solution for release, the free BSA would diffuse out of the nanoporous multilayers to gradually shift the balance of Reaction 2 to the left. Furthermore, the much higher concentration of neighboring uncomplexed alginate could form a strong competition by combining with PEI to exchange BSA from PEI:BSA complex, thus continuously driving BSA to release. Indeed, the ratio of alginate to PEI plays a dominant role in the release of BSA, of which a higher ratio of alginate to PEI at lower assembly pH favors more thorough release of BSA (Figure 5). The possible molecular process of reversible protein loading and release is illustrated in **Scheme 1**.

### 2.3. Controlled Protein Loading and Release Capability

From **Figure 6**, it can be seen that the loaded FITC-BSA increases exponentially with increase of the bilayer number, indicating that protein can penetrate into the multilayers and the loading capacity of the film can be greatly enhanced by simply increasing the bilayer number. In contrast, as a control, the conventional linearly growing PDDA/PSS multilayers assembled in PBS solution has much lower loading and no increase is observed with increasing the bilayer number of PDDA/PSS multilayers due to their dense and immobile structure.[42,63] Notably, the measured loading

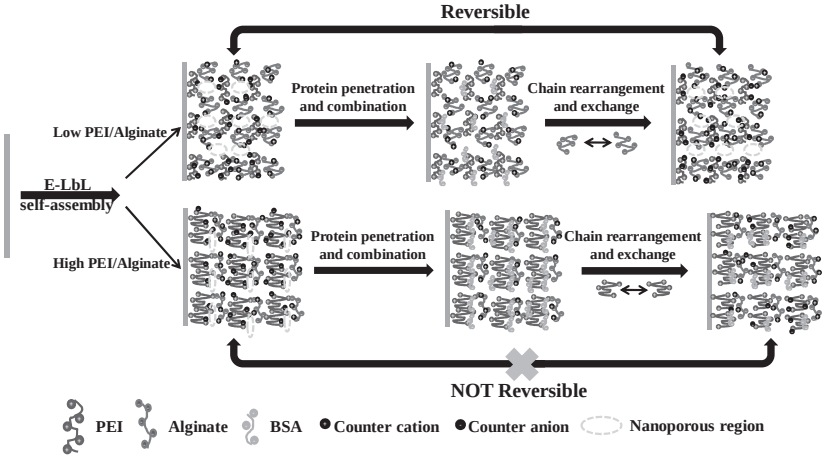


**Scheme 1.** Possible molecular process of reversible protein loading and release.

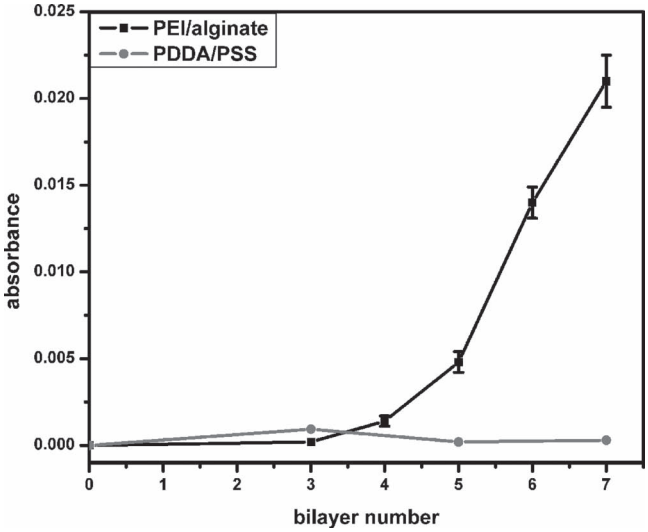


**Figure 6.** Comparison of loading amount of FITC-BSA in PEI/alginate multilayers and PDDA/PSS multilayers with different bilayer number.

capacity for 5-bilayer film is as high as 2.54 μg $cm^{-2}$. To our knowledge, this is the highest loading capacity for reported BSA loading systems.[64,65] This value is much higher than the surface density of close-packed monolayer of BSA with end-on configuration (around 0.88 μg $cm^{-2}$),[65,66] and can be further increased exponentially by increasing the bilayer number, as shown in Figure 6.

The sustained release property of the protein-loaded multilayers assembled at pH 5 was further studied (**Figure 7**), showing that the release can be easily controlled by the bilayer number. In particular, the release process for different bilayered films has the same trend, with different release times and both surface and cumulative release time being increased with the number of bilayers, indicating good controllability. For the 5-bilayer multilayered film, the release can be sustained for around 565 min, while the release for the 15-bilayer film is remarkably increased to 40 d, at least, which is the longest protein release time reported for LbL-assembly films,[11,67] and could be further increased by further increasing the bilayer number. The extremely long release time should also be ascribed to the nanoporous structures, which could significantly increase the diffusion length and reduce the release rate.[34–36] The good controllability by the bilayer number for a wide range of release time provides a broad range of potential applications. With high loading capacity and good reversibility, the fast release can be well used in protein separation and biocatalysis,[14,17] while the long sustainable release can offer great potential in protein delivery applications.[68]

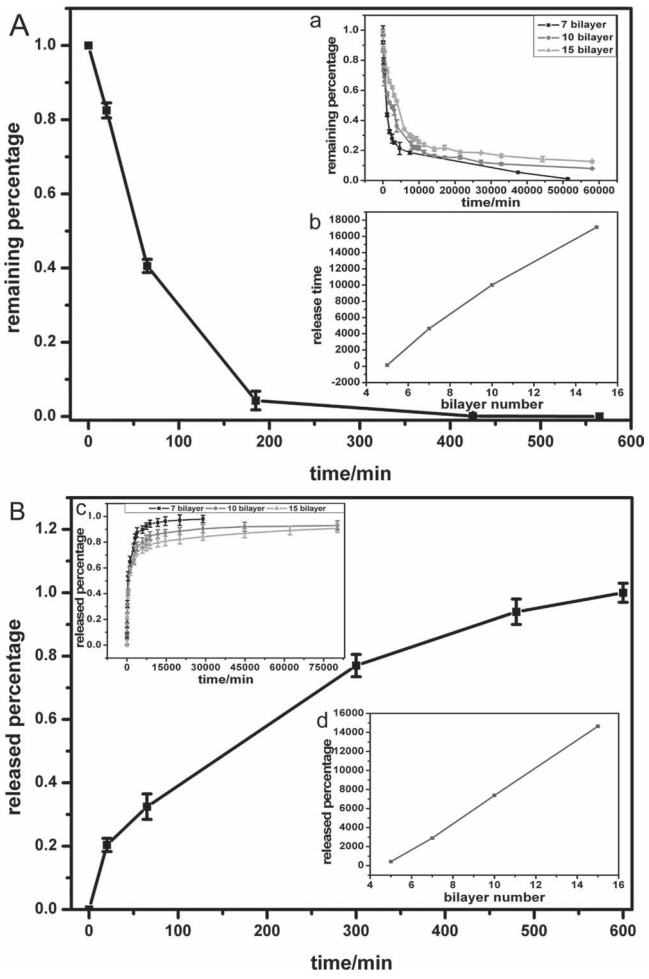


**Figure 7.** A) Surface release kinetics of FITC-BSA from PEI/alginate multilayers with 5 bilayers. The remaining percentage is calculated by dividing the remaining UV-vis peak intensity by the original UV-vis peak intensity. Insets show the release kinetics of multilayers with higher bilayer number (a) and the release time needed to achieve remaining percentage of 20% versus bilayer number (b). B) Cumulative release of FITC-BSA for PEI/alginate multilayers with 5 bilayers obtained by measuring the florescence of solution. Insets show the cumulative release for multilayers with other bilayer number (c) and the release time needed to achieve 80% release versus bilayer number (d).

## 3. Conclusions

In conclusion, a novel ultrafast exponentially growing nanoporous multilayered film has been assembled from two weak polyelectrolytes, PEI and alginate with thickness and chemical composition controlled by the assembly pH. For the first time, the assembled film demonstrates stimuli-free reversible loading and release of protein at physiological conditions by a synthetic material, while accomplishing the highest loading capacity and longest release time for an LbL-assembled film up to date. With great tunability of multilayer properties at a molecular level through selecting a broad range of building blocks and controlling assembly conditions for expected internal structure and chemical composition, this method can be widely extended for reversible loading and release of various biofunctional proteins with extremely high protein loading capability, excellent reversibility, and controllable ultralong release time at physiological conditions, thus providing great potentials to deliver proteins for various important biomedical applications.

## 4. Experimental Section

*Chemicals*: PEI (branched, 50% in water, $\overline{M}_w$ 750 000), alginate (sodium salt, 20–40 cP, 1% in $H_2O$), BSA (minimum 98%, electrophoresis), and fluorescein isothiocyanate (FITC) (HPLC, 90%) were all purchased from Sigma-Aldrich. Deionized (DI) water was prepared from a Millipore Milli-Q water purification system. FITC-labeled BSA (FITC-BSA) was prepared by mixing BSA and FITC at a molar ratio of 1:1 in $Na_2CO_3$–$NaHCO_3$ buffer for 2 h, followed by thorough dialysis in pH 7.4 PBS for 1 month. FITC-labeled PEI was prepared according to the literature.[45] The PEI PBS solution and alginate PBS solution with desired pH was prepared by dissolving PEI and alginate in pH-adjusted buffer solution. The pH values of PBS were adjusted by HCl (1 M) or NaOH (1 M). Glass slides and silicon wafers were cleaned by immersing in freshly prepared piranha solution ($H_2SO_4/H_2O_2$ 7:3, v/v) until no bubbles could be observed, followed by thorough rinsing with DI water. $CaF_2$ sheets were cleaned by ultrasonicating sequentially in acetone, ethanol, and DI water for 15 min each.

*Assembly of PEI/Alginate Multilayer Films*: Cleaned glass slides or silicon wafers were immersed into PEI PBS solution (1 mg $mL^{-1}$) with predetermined pH for 15 min, followed by washing with PBS at the same pH 5 times and then drying under $N_2$ flow. Subsequently, the substrates were immersed into alginate PBS solution (1 mg $mL^{-1}$, the same pH) for 15 min, and then rinsed with PBS (the same pH) 5 times and dried under $N_2$ flow. The procedure was repeated several times to obtain PEI/alginate multilayer films. The multilayer film obtained by *n*-times of repeats is denoted as $(PEI/alginate)_n$.

*Loading and Release of FITC-BSA*: For loading FITC-BSA, PEI/alginate multilayer films were immersed into BSA PBS solution (1 mg $mL^{-1}$) for 12 h, rinsed with PBS (pH 7.4) 3 times and then blown dry with $N_2$. For the release of FITC-BSA, FITC-BSA loaded PEI/alginate multilayer films were immersed in PBS (pH 7.4) for a predetermined time period, during which the release solution was frequently refreshed to ensure the constant release condition. The incubation temperature was 37 °C. The BSA concentration in PBS after thorough release was measured by both the micro-BCA method and using a fluorospectrometer (Nanodrop 3300) to determine the loading capacity of multilayers. The loading and release of FITC-BSA was monitored by measuring the absorbance of the FITC-BSA loaded PEI/alginate multilayer film via UV-vis spectroscopy using a UV-2450 spectrometer, and the fluorescence of the PBS solution after release via a fluorospectrometer (Nanodrop 3300). To obtain the net absorbance of FITC-BSA, baseline correction was performed for FITC-BSA loaded PEI/alginate multilayers. The fluorescence images of multilayer assembled glass slides with/without FITC-BSA loaded and after FITC-BSA release were obtained from a ProXPRESS 2D Proteomic Imaging System.

*Characterization*: The FE-SEM and cross-section FE-SEM images of PEI/alginate multilayer films were obtained from a JEOL (JSM-6700F) microscope at an acceleration voltage of 5 kV and a working distance of about 8 mm. The Cryo-TEM imaging was carried out with a FEI Tecnai T12 microscope at 120 kV. The cross-section CLSM imaging was performed with a Carl Zeiss LSM 510 META confocal microscope. The chemical composition of PEI/alginate multilayer films was examined by a FTIR spectrometer (PerkinElmer, Spectrum GX) and depth profiling XPS using Kratos AXIS spectrometer with monochromatic Al K (1486.71 eV) X-ray radiation (15 kV and 10 mA). Pristine $CaF_2$ sheet was used as the substrate for FTIR spectroscopy. The absorption curves were recorded after assembly of each bilayer. The assembly process on $CaF_2$ sheet was the same as that on glass slide or silicon wafer. For the depth profiling XPS, Ar ion bombardment was carried out using a differential pumping ion gun (Kratos MacroBeam) with an accelerating voltage of 4 keV. The bombardment was performed at an angle of incidence of 45° with respect to the surface normal.

*Experimental Details*: See the Supporting Information for further experimental details.

## Supporting Information

Supporting Information is available from the Wiley Online Library or from the author.

## Acknowledgements

This work was financially supported by the Institute for Clean Energy & Advanced Materials, Southwest University, P. R. China, and the Center for Advanced Bionanosystems, Nanyang Technological University, Singapore.

Received: September 27, 2011
Revised: November 19, 2011
Published online: February 8, 2012

[1] X. Cao, M. E. Pettitt, F. Wode, M. P. A. Sancet, J. Fu, J. Ji, M. E. Callow, J. A. Callow, A. Rosenhahn, M. Grunze, *Adv. Funct. Mater.* **2010**, *20*, 1984.
[2] M. E. McConney, K. D. Anderson, L. L. Brott, R. R. Naik, V. V. Tsukruk, *Adv. Funct. Mater.* **2009**, *19*, 2527.
[3] V. Gopishetty, Y. Roiter, I. Tokarev, S. Minko, *Adv. Mater.* **2008**, *20*, 4588.
[4] Z. Wang, J. Zhang, J. Xie, C. Li, Y. Li, S. Liang, Z. Tian, T. Wang, H. Zhang, H. Li, W. Xu, B. Yang, *Adv. Funct. Mater.* **2010**, *20*, 3784.
[5] Q. Fu, E. Saiz, A. P. Tomsia, *Adv. Funct. Mater.* **2011**, *21*, 1058.
[6] J. S. Mohammed, W. L. Murphy, *Adv. Mater.* **2009**, *21*, 2361.
[7] S. An, R. Kumar, E. D. Sheets, S. J. Benkovic, *Science* **2008**, *320*, 103.
[8] D. M. Gakamsky, I. F. Luescher, I. Pecht, *Proc. Natl. Acad. Sci. USA* **2004**, *101*, 9063.
[9] P. Bernadó, T. Åkerud, J. García de la Torre, M. Akke, M. Pons, *J. Am. Chem. Soc.* **2002**, *125*, 916.
[10] L. Wang, X. Wang, M. Xu, D. Chen, J. Sun, *Langmuir* **2008**, *24*, 1902.
[11] E. Kharlampieva, I. Erel-Unal, S. A. Sukhishvili, *Langmuir* **2006**, *23*, 175.
[12] C.-C. Lin, A. Metters, *Pharmacol. Res.* **2006**, *23*, 614.
[13] B. Mattiasson, A. Kumar, A. E. Ivanov, I. Y. Galaev, *Nat. Protocols* **2007**, *2*, 213.
[14] L. Mu, Y. Liu, S. Cai, J. Kong, *Chem.–Eur. J.* **2007**, *13*, 5113.
[15] M. L. O'Grad, K. K. Parker, *Langmuir* **2007**, *24*, 316.
[16] G. Zhen, D. Falconnet, E. Kuennemann, J. Voros, N. D. Spencer, M. Textor, S. Zurcher, *Adv. Funct. Mater.* **2006**, *16*, 243.
[17] T. Montes, V. Grazu, F. López-Gallego, J. A. Hermoso, J. M. Guisán, R. Fernández-Lafuente, *Biomacromolecules* **2006**, *7*, 3052.
[18] P. Wan, Y. Wang, Y. Jiang, H. Xu, X. Zhang, *Adv. Mater.* **2009**, *21*, 4362.
[19] P. Sharma, S. Garg, *Adv. Drug Delivery Rev.* **2010**, *62*, 491.
[20] J. P. Schillemans, E. Verheyen, A. Barendregt, W. E. Hennink, C. F. Van Nostrum, *J. Controlled Release* **2011**, *150*, 266.
[21] M. Müller, B. Kessler, H.-J Adler, K. Lunkwitz, *Macromol. Symp.* **2004**, *210*, 157.
[22] G. Jenikova, U. L. Lao, D. Gao, A. Mulchandani, W. Chen, *Langmuir* **2007**, *23*, 2277.
[23] S. Saksena, A. L. Zydney, *Biotechnol. Bioeng.* **1994**, *43*, 960.
[24] K. Thornton, A. M. Smith, C. L. R. Merry, R. V. Ulijn, *Biochem. Soc. Trans.* **2009**, *037*, 660.
[25] J. Zhang, L. S. Chua, D. M. Lynn, *Langmuir* **2004**, *20*, 8015.
[26] E. Vázquez, D. M. Dewitt, P. T. Hammond, D. M. Lynn, *J. Am. Chem. Soc.* **2002**, *124*, 13992.
[27] F. Tristan, G. Palestino, J. L. Menchaca, E. Perez, H. Atmani, F. Cuisinier, G. Ladam, *Biomacromolecules* **2009**, *10*, 2275.
[28] D. S. Salloum, J. B. Schlenoff, *Biomacromolecules* **2004**, *5*, 1089.
[29] Q. Li, J. F. Quinn, Y. Wang, F. Caruso, *Chem. Mater.* **2006**, *18*, 5480.
[30] N. S. Zacharia, M. Modestino, P. T. Hammond, *Macromolecules* **2007**, *40*, 9523.
[31] H. W. Jomaa, J. B. Schlenoff, *Langmuir* **2005**, *21*, 8081.
[32] J. K. Lim, S. A. Majetich, R. D. Tilton, *Langmuir* **2009**, *25*, 13384.

[33] A. J. Chung, M. F. Rubner, *Langmuir* **2002**, *18*, 1176.
[34] M. C. Berg, L. Zhai, R. E. Cohen, M. F. Rubner, *Biomacromolecules* **2006**, *7*, 357.
[35] D. A. Bernards, T. A. Desai, *Soft Matter* **2010**, *6*, 1621.
[36] W. Yuan, C. M. Li, *Chem. Commun.* **2010**, *46*, 9161.
[37] P. Podsiadlo, M. Michel, J. Lee, E. Verploegen, N. Wong Shi Kam, V. Ball, J. Lee, Y. Qi, A. J. Hart, P. T. Hammond, N. A. Kotov, *Nano Lett.* **2008**, *8*, 1762.
[38] P. J. Yoo, N. S. Zacharia, J. Doh, K. T. Nam, A. M. Belcher, P. T. Hammond, *ACS Nano* **2008**, *2*, 561.
[39] S. Srivastava, V. Ball, P. Podsiadlo, J. Lee, P. Ho, N. A. Kotov, *J. Am. Chem. Soc.* **2008**, *130*, 3748.
[40] C. Picart, J. Mutterer, L. Richert, Y. Luo, G. D. Prestwich, P. Schaaf, J.-C. Voegel, P. Lavalle, *Proc. Natl. Acad. Sci. USA* **2002**, *99*, 12531.
[41] N. S. Zacharia, D. M. DeLongchamp, M. Modestino, P. T. Hammond, *Macromolecules* **2007**, *40*, 1598.
[42] P. Lavalle, J. C. Voegel, D. Vautier, B. Senger, P. Schaaf, V. Ball, *Adv. Mater.* **2011**, *23*, 1191.
[43] J. Fu, J. Ji, L. Shen, A. Kueller, A. Rosenhahn, J. Shen, M. Grunze, *Langmuir* **2008**, *25*, 672.
[44] I. Choi, R. Suntivich, F. A. Plamper, C. V. Synatschke, A. H. E. Muller, V. V. Tsukruk, *J. Am. Chem. Soc.* **2011**, *133*, 9592.
[45] W. Yuan, Z. Lu, C. M. Li, *J. Mater. Chem.* **2011**, *21*, 5148.
[46] J. T. Wilson, W. Cui, V. Kozlovskaya, E. Kuarlampieva, D. Pan, Z. Qu, V. R. Krishnamurthy, J. Mets, V. Kumar, J. Wen, Y. Song, V. V. Tsukruk, E. L. Chaikof, *J. Am. Chem. Soc.* **2011**, *133*, 7054.
[47] K. Ren, T. Crouzier, C. Roy, C. Picart, *Adv. Funct. Mater.* **2008**, *18*, 1378.
[48] L. Lebrun, F. Vallee, B. Alexandre, Q. T. Nguyen, *Desalination* **2007**, *207*, 9.
[49] X. X. Liu, L. Y. Qian, T. Shu, Z. Tong, *Polymer* **2003**, *44*, 407.
[50] S. S. Shiratori, M. F. Rubner, *Macromolecules* **2000**, *33*, 4213.
[51] L. Richert, P. Lavalle, E. Payan, X. Z. Shu, G. D. Prestwich, J. F. Stoltz, P. Schaaf, J. C. Voegel, C. Picart, *Langmuir* **2004**, *20*, 448.
[52] P. Kujawa, P. Moraille, J. Sanchez, A. Badia, F. M. Winnik, *J. Am. Chem. Soc.* **2005**, *127*, 9224.
[53] F. Boulmedais, V. Ball, P. Schwinte, B. Frisch, P. Schaaf, J. C. Voegel, *Langmuir* **2003**, *19*, 440.
[54] C. Porcel, P. Lavalle, G. Decher, B. Senger, J. C. Voegel, P. Schaaf, *Langmuir* **2007**, *23*, 1898.
[55] B. Schoeler, G. Kumaraswamy, F. Caruso, *Macromolecules* **2002**, *35*, 889.
[56] X. Cui, R. Pei, Z. Wang, F. Yang, Y. Ma, S. Dong, X. Yang, *Biosens. Bioelectron.* **2003**, *18*, 59.
[57] B. Sarmento, D. Ferreira, F. Veiga, A. Ribeiro, *Carbohydr. Polym.* **2006**, *66*, 1.
[58] H. F. Shi, Y. Zhao, X. Q. Zhang, S. C. Jiang, D. J. Wang, C. C. Han, D. F. Xu, *Macromolecules* **2004**, *37*, 9933.
[59] B. S. Kim, J. M. Oh, K. S. Kim, K. S. Seo, J. S. Cho, G. Khang, H. B. Lee, K. Park, M. S. Kim, *Biomaterials* **2009**, *30*, 902.
[60] F. van de Manakker, K. Braeckmans, N. el Morabit, S. C. De Smedt, C. F. van Nostrum, W. E. Hennink, *Adv. Funct. Mater.* **2009**, *19*, 2992.
[61] P. Nazaran, V. Bosio, W. Jaeger, D. F. Anghel, R. von Klitzing, *J. Phys. Chem. B* **2007**, *111*, 8572.
[62] N. Laugel, C. Betscha, M. Winterhalter, J.-C. Voegel, P. Schaaf, V. Ball, *J. Phys. Chem. B* **2006**, *110*, 19443.
[63] R. A. McAloney, M. Sinyor, V. Dudnik, M. C. Goh, *Langmuir* **2001**, *17*, 6655.
[64] B. Saha, G. Das, *J. Phys. Chem. C* **2009**, *113*, 15667.
[65] M. Espanol, R. A. Perez, E. B. Montufar, C. Marichal, A. Sacco, M. P. Ginebra, *Acta Biomater.* **2009**, *5*, 2752.
[66] S. J. McClellan, E. I. Franses, *Colloids Surf., B* **2003**, *28*, 63.
[67] L. J. De Cock, S. De Koker, F. De Vos, C. Vervaet, J.-P Remon, B. G. De Geest, *Biomacromolecules* **2010**, *11*, 1002.
[68] M. Macdonald, N. M. Rodriguez, R. Smith, P. T. Hammond, *J. Controlled Release* **2008**, *131*, 228.